Published in IET Microwaves, Antennas & Propagation
Received on 7th August 2013
Revised on 26th February 2014
Accepted on 19th March 2014
doi: 10.1049/iet-map.2013.0432

ISSN 1751-8725

Reflectarray antenna based on grounded loop-wire miniaturised-element frequency selective surfaces

Arezou Edalati, Kamal Sarabandi

EECS Department, Radiation Laboratory (RadLab), University of Michigan, 3228 EECS Building, 1301 Beal Avenue, Ann Arbor, MI 48109-2122, USA
E-mail: arezoued@gmail.com

Abstract: A reflectarray antenna based on a metal-backed co-planar loop-wire Miniaturized Element Frequency Selective Surface (MEFSS) is presented in this paper. Since the unit cells are small compared to the wavelength, an equivalent lumped-element model can describe the spectral behaviour of the proposed MEFSS structure. It is shown that the proposed unit cell provides a wider and gentler phase variation as a function of the loop size compared to a metallic patch or loop element and that the phase response of the loop-wire element has very low sensitivity to the angle of incidence. In addition, the response of the unit cell, to a great extent, depends on the geometric and electrical parameters of the cells themselves with minimum dependency on the neighbouring elements and therefore the reflected signal phase can be controlled locally. Three samples of the proposed MEFSS structure, each giving different reflection phase values, are fabricated and measured to validate the circuit model and the design procedure. A prototype MEFSS-based reflectarray antenna at X-band is fabricated and measured. The prototype (260 mm × 260 mm and F/D = 1.02) shows a maximum gain of 26.3 dBi with a 1 dB-gain bandwidth of 17% and 3-dB beamwidth of 6° in agreement with the design parameters.

1 Introduction

High-gain, low-cost and conformal antennas are highly desirable for many communication and radar applications such as satellite and point-to-point communications as well as terrestrial and avionic radar systems. The conventional parabolic reflector antennas have been used widely because of their high-gain characteristic [1]; however, because of their three-dimensional structure, they require significant volume on their platform. As an alternative solution, flat phased-array antennas have been utilised in many applications as a substitution for the parabolic reflectors [2]. One drawback of phased-array antennas is the losses in their corporate feed which reduce the antenna efficiency (gain) substantially. As a remedy, flat printed reflectarray antennas have become an attractive alternative solution to both the conventional parabolic reflector and phased-array antennas. They have several advantages such as high gain, flatness, low loss, low cost, low volume and less manufacturing complexity [3–7].

The major drawback of reflectarray antennas is their narrow bandwidth. Different approaches have been introduced and employed to enhance the bandwidth of the reflectarray antennas. These include implementation using a multilayer substrate with stacked resonance elements [8, 9], single layer with multi-resonance elements [10–14], reflectarray with sub-wavelength unit cells [15–19] and multi-layer structure with sub-wavelength elements [20]. However, stacking reflectarray elements in the multilayer substrate need complex fabrication processes which often lead to higher cost. On the other hand, miniaturising reflectarray elements is also challenging, because to achieve the desired reflected phase span of 360° is not always achievable and the phase variation as a function of element dimension is fast because of higher quality factor of such resonators. The latter leads to tight fabrication tolerance which makes the fabrication process more complicated. To design sub-wavelength reflectarray elements with the maximum phase range and smooth phase variation against change in structural dimensions, elements with higher order frequency response are needed.

Metallic patch and loop elements have been widely studied and employed as a reflectarray unit cells with resonant or sub-wavelength size. In [19], it has been shown that the sub-wavelength loop element has the advantage of providing a wider phase span compared to a patch unit cell with the same size. This makes the loop structure a better choice for designing the reflectarray antenna. In this paper, a sub-wavelength element with higher order frequency response is considered. It is shown that a single-layer loop-wire sub-wavelength element provides wider phase range compared to patch or loop alone with the same size. This element also shows a lower sensitivity to the wave angle of incidence compared to the loop element, and provides a smooth phase variation against structural dimensions. These characteristics make the loop-wire sub-wavelength element a better choice for designing reflectarray antennas.

Miniaturised-element frequency selective surface (MEFSS) elements with periodicity much smaller than a wavelength

have been introduced recently [21] with notable advantage compared to the conventional FSS such as minimal mutual coupling between elements, localised frequency response, low dependency to the incident angle, existence of an equivalent circuit model, TEM mode operation and harmonic free frequency response. In [22], MEFSS structures are proposed as multipole spatial filters. Here, as a new application for MEFSS, a printed single-sided MEFSS structure backed with a ground plane is chosen for designing a reflectarray antenna. The building block of the MEFSS is formed by a wire grid and a metallic loop inside of it on top of a metallic surface. By changing the dimension of the square metallic loop, the phase of the transmission coefficient through the MEFSS and as a result, the total reflection coefficient at the operating frequency is modified. By proper placement of cells with a predetermined phase characteristics across the surface, the spherical curvature of the incident wave phase front can be corrected to create an antenna with a narrow beam in a desired direction. The proposed reflectarray antenna is designed to operate at the X-band. The antenna with total dimensions of 260 mm × 260 mm and $F/D = 1.02$ is fabricated and measured in the anechoic chamber of the University of Michigan.

In Section 2, the design method and the equivalent circuit of the loop-wire MEFSS element are presented. In addition, to show the advantages of the proposed unit cell compared to the patch and loop elements, their phase characteristics are presented and compared. To validate the circuit model performance, three MEFSS unit cells for operation in a rectangular waveguide are fabricated and the measured results are compared with the circuit model and a full-wave simulation. In addition, a parametric study is carried out to examine the effects of the geometrical parameters on the metal-backed loop-wire MEFSS response. In Section 3, the design procedure for the reflectarray antenna is described and the measurement results are shown and compared with the simulation results. Finally, concluding remarks are given in Section 4.

2 Design of the unit cell and its characteristics

The concept of the operation is based on utilising the phase shift a wave experiences as it goes through a spatial filter. Basically if the frequency of the signal is slightly lower or higher than the centre frequency of the filter the output signal experiences a phase lag or a phase lead. Reflecting back the transmitted signal using a mirror (ground plane behind the spatial filter) the phase shift can be doubled. For a reflectarray spatially varying phase across the reflectarray is required. This is done by scaling the dimensions of the unit cells as described below.

For this application, we consider a single-sided (co-planar) loop-wire MEFSS structure. To show the advantage of the proposed unit cell compared to the widely used patch or loop element, their phase characteristics are presented and compared. The unit cell of the loop-wire, loop and patch elements is shown in Fig. 1. All three unit cells have the same periodicity of W_x, same substrate with permittivity of $\varepsilon_r = 2.2$, a thickness of $h_{sub} = 3.175$ mm and they are backed with a ground plane. Typical dimensions of the unit cells are presented in Table 1. The length of W_2 is modified to achieve the required phase shift for designing the reflectarray antenna.

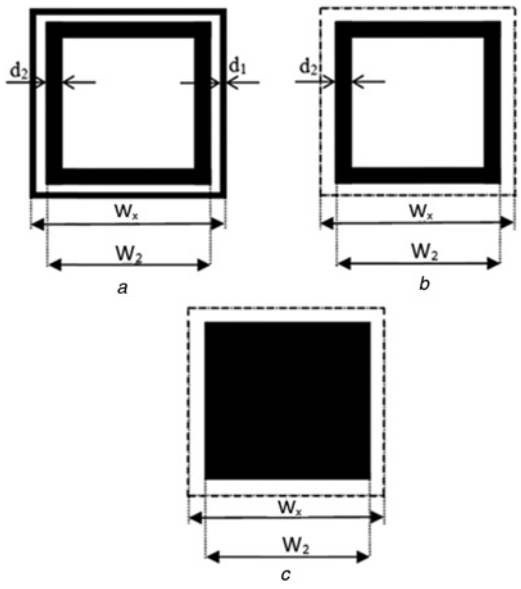

Fig. 1 *Unit cell*

a Grounded loop-wire element
b Grounded loop element
c Grounded patch element (all unit cells have the same periodicity of W_x and the same substrate)

Table 2 presents the maximum reflected phase variation when W_2 is changed for the three unit cells of Fig. 1 at 10.7 GHz and for two values of period ($W_x = 15$ and 10 mm). As it can be seen, by miniaturising the elements, the maximum phase-span decreases. In addition, loop-wire provides notably larger phase variation compared to the loop and patch elements having the same size. As presented, the peak-to-peak phase variation of the loop-wire structure for $W_x = 10$ mm is about 50° and 90° more than what can be achieved from the loop and patch structures, respectively. This means that using the loop-wire elements to design a reflectarray antenna, the phase error, defined as 360° – the total phase span provided by reflectarray elements, is $< 20°$, whereas this error is 70° and 110° for the loop and patch structure, respectively.

It has been shown that the interaction of MEFSS structures with incoming incident plane waves is predominantly in TEM mode [21]; therefore, an equivalent circuit model can be found for each unit cell to describe the physics behind the operation of the proposed structure.

Table 1 Unit cell dimensions (millimetre)

d_1	W_x	ε_r	h_{sub}
0.08	10	2.2	3.175

Table 2 Phase span of different reflectarray elements

	$h_{sub} = 3.175$ mm, $d_2 = 0.9$ mm, $\varepsilon_r = 2.2$ freq = 10.7 GHz	
	$W_x = 15$ mm	$W_x = 10$ mm
patch	255°	250°
loop	315°	290°
loop wire	350°	340°

doi: 10.1049/iet-map.2013.0432

To find the equivalent circuit model of each structure, each element is assumed in a square unit cell composed of parallel perfect electric conductors (PECs) (perpendicular to the electric field) and a pair parallel perfect magnetic conductors (PMCs) (perpendicular to the magnetic field). Such a unit cell can be viewed as a waveguide that can support TEM waves. The application of image theory will reproduce the original periodic structure with a plane wave illumination. Assuming a plane wave illumination with the ***E***-field vector in the x-direction, for the loop-wire unit cell, the gaps between the wire and the loop can be represented by a capacitor C_1. The vertical metallic traces of the loop and the wire grid can be modelled by inductors represented by L_1 and L_2, respectively. There is also a significant mutual coupling between the wire and loop which is represented with the coupling coefficient K in the circuit model. The effect of the substrate and the ground plane is modelled with a short-circuit transmission line, as presented in Fig. 2*a*. The equivalent circuit model for patch and loop structures is the same, a series LC circuit as presented in Fig. 2*b*; however, the patch inductance is very small and almost negligible compared to the inductance of the loop element. By comparing the circuit model of the proposed elements, it can be understood that the additional inductance of the wire (L_2) and the magnetic coupling between the loop and wire in the loop-wire structure creates a higher order pass-band frequency response, which enhances the performance of the loop-wire element in achieving a larger phase span.

To achieve the required phase shift, the length of the metallic square loop (the length of the patch in the patch unit cell) is modified. Therefore the inductance L_1, the gap capacitance of C_1 and the mutual coupling between the wire and the metallic loop are changed (in the loop structure, the inductance of L, the gap capacitance of C and in the patch structure the gap capacitance of C are modified). This way the phase of the reflection coefficient can be tuned.

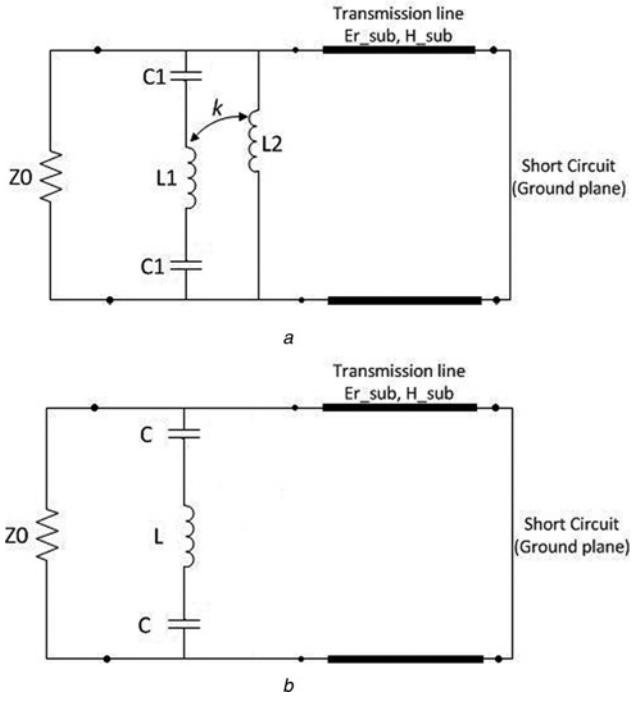

Fig. 2 *Equivalent circuit model*

a Grounded loop-wire MEFSS
b Grounded loop and patch elements

The initial values of the equivalent circuit model are extracted from the following equations [23]; however, these analytical expressions are not exact because of the finiteness of the metallic strips that make the loops and wire mesh. The corrections to these calculations are obtained from the curve fitting between the circuit model and full-wave simulation. The curve fitting is needed to adjust for the effects of corners and truncations

$$C_1 = \varepsilon_0 \epsilon_{\text{eff}} \frac{2W_2}{\pi} \log\left(\frac{1}{\sin(\pi s/2W_2)}\right) \tag{1}$$

$$L_1 = \mu_0 \frac{W_2}{2\pi} \log\left(\frac{1}{\sin(\pi d_2/2W_2)}\right) \tag{2}$$

$$L_2 = \mu_0 \frac{W_x}{2\pi} \log\left(\frac{1}{\sin(\pi d_1/2W_x)}\right) \tag{3}$$

$$S = W_x - W_2 - d_1 \tag{4}$$

To show the accuracy of the circuit model and the design process, three different unit cells of the loop-wire structure, all having the same periodicity and only changing the loop-length (W_2) parameter, are designed, fabricated and tested using the standard WR90 X-band waveguide. In this case the period of the metal-backed MEFSS is chosen so that it would commensurate the waveguide cross-sectional dimensions. The waveguide support TE_{10} mode and thus the MEFSS can be viewed as being illuminated by two plane waves, having two equal but opposite lateral ***k***-vectors and equal longitudinal ***k***-vectors, at oblique incidence. Fig. 3 shows the fabricated unit cells. The other side of the test waveguide is connected to a vector network analyser through a waveguide to the co-axial line adaptor. The network analyser and the test waveguide were calibrated with the reference plane at the open surface of the waveguide using short, offset short and matched loads [24]. The measured results of the magnitude and phase of the reflection coefficients for three samples are compared with the equivalent circuit model and the full-wave simulation are shown in Fig. 4. The equivalent lumped-element values for fabricated unit cells are presented in Table 3. Good agreement is observed between the circuit model, the full-wave simulation and the measurement results which show the accuracy of the circuit model and the design procedure. In addition, as shown in Fig. 4*b*, the magnitude of the reflection coefficient for all three samples of MEFSS is < 0.4 dB which shows the low-loss performance of the MEFSS elements.

It is important to note that the principle of operation of the loop-wire elements is also different from an array of

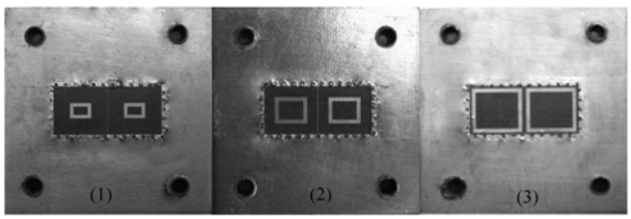

Fig. 3 *Photograph of the fabricated loop-wire unit cells*

$W_x = 11.43$ mm, $W_y = 10.16$ mm, $d_1 = 0.08$ mm, $d_2 = 0.9$ mm, $W_{2(\text{FSS1})} = 3.24$ mm, $W_{2(\text{FSS2})} = 5.52$ mm, $W_{2(\text{FSS3})} = 9.24$ mm

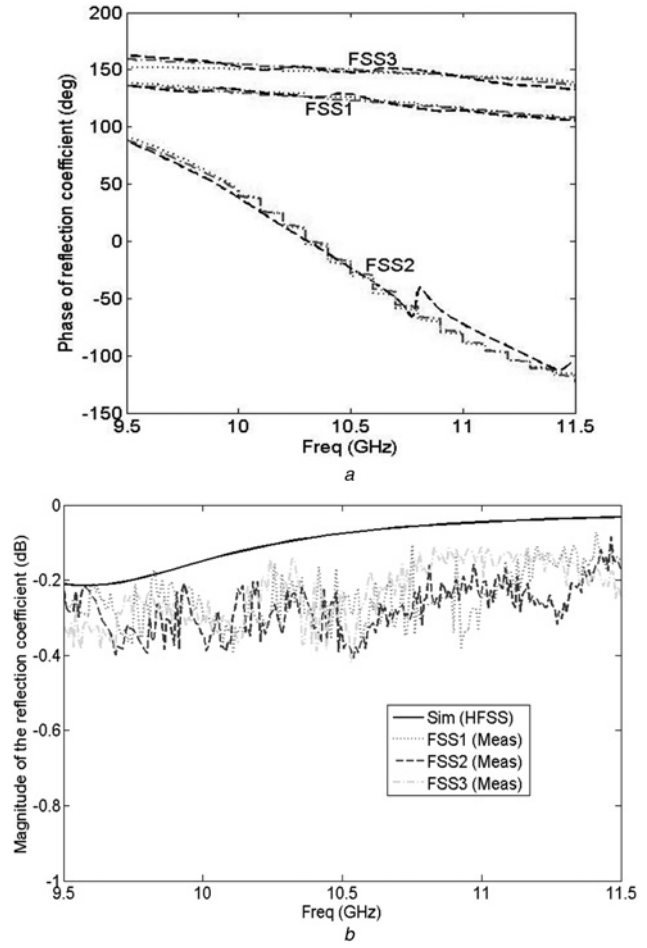

Fig. 4 *Magnitude and phase of the reflection coefficients of three MEFSS samples*

a Phase of the reflection coefficient for three MEFSS samples ('-.' HFSS, ':' ADS circuit model, '–' measurement)
b Magnitude of the reflection coefficient ('solid line' HFSS, '…' FSS1, '——' FSS2, '–.–'FSS3)

concentric loops [10, 13]. Concentric loops have multi-resonance characteristic which is not the case in the loop-wire elements. Indeed, the loop-wire elements, compared to an array of single loops, has higher order filtering response because of the additional inductance and coupling between the two branches, but, they have a lower filtering response compared to the array of concentric loops.

The effect of the wave angle of incidence (at 0, 30°, 45°) on the phase of the reflection coefficient for the loop and loop-wire elements with their resonant dimensions is presented and compared in Fig. 5. As shown, the phase of the reflection coefficient of the loop-wire element shows less sensitivity to the angle of incidence, especially for the TM polarisation when compared to the loop elements alone. In addition, the phase of the reflection coefficient of the loop-wire unit cell against various loop lengths for three different angles of incidence and TE/TM polarisation at 10.7 GHz are presented in Fig. 6. As illustrated, the

Table 3 Equivalent circuit model values

	FSS1	FSS2	FSS3
C_1, fF	31.6	67	99.3
L_1, nH	2.64	3.61	6.4
L_2, nH	2	2	2
k	−0.99	−0.51	0.69

sensitivity of the proposed structure to the polarisation and incident angle is very low. This allows a very simple design procedure for the reflectarray antenna since the reflectarray elements are simply designed based on their normal incidence characteristics.

To show the effects of different design parameters on the phase of the reflection coefficient of the proposed loop-wire unit cell, a parametric study is carried out and the results are presented in Figs. 7 and 8. These figures show the effects of the width of the wire (d_1) and width of the loop (d_2) on the phase of the reflection coefficients for various loop-length dimensions. As shown, narrower wire width and wider loop width give a smoother phase variation against the loop length dimension.

3 Reflectarray antenna design and measurement eesults

The arrangement of MEFSS unit cells with different phase responses across the reflectarray can be set in the manner to modify the phase front of an incident wave to any desired form. For example, if the incident wave has a spherical phase front (generated from a point source at the focal

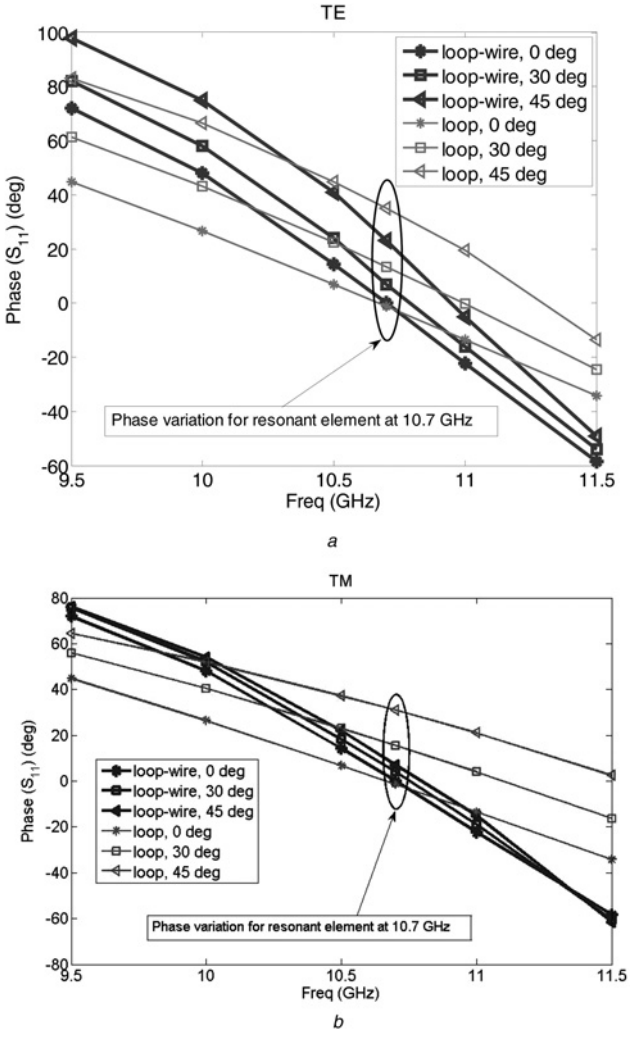

Fig. 5 *Effect of the angle of the incidence (θ) on the phase of the reflection coefficient for the resonant element of loop (W_2 = 5.2 mm) and loop wire (W_2 = 5.7 mm)*

a TE mode
b TM mode

doi: 10.1049/iet-map.2013.0432

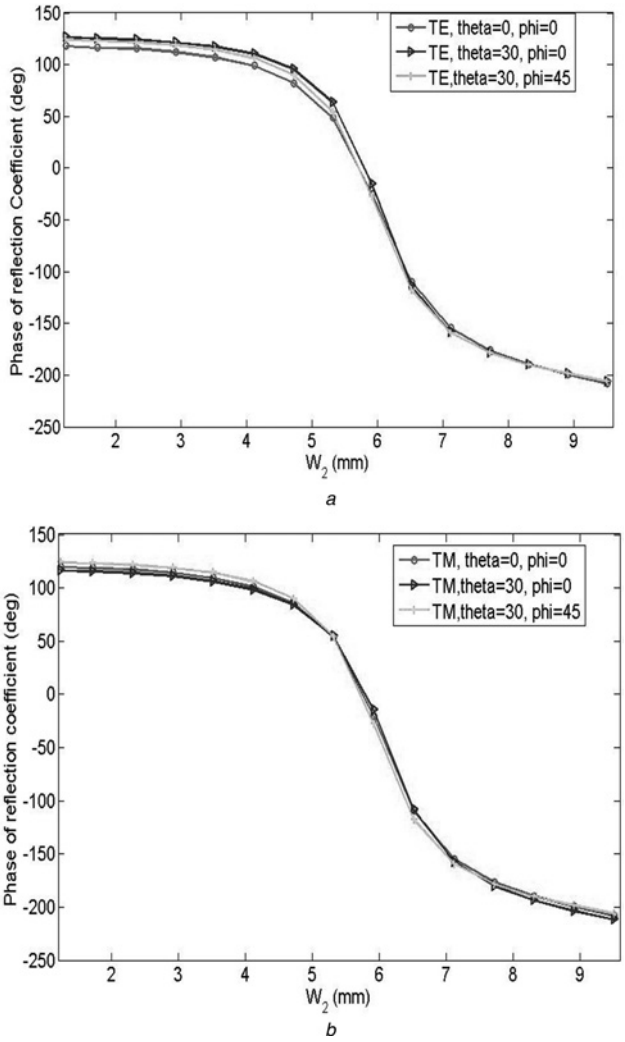

Fig. 6 *Phase of the reflected wave against loop length for three angles of incidence at 10.7 GHz*

a TE mode
b TM mode

point), the phase response of each unit cell can be chosen to compensate the incident phase delay associated with the path length difference compared to the centre element. This way the reflectarray will turn a spherical phase front to a planar phase front which can generate a narrow beam. This is a standard approach used for all reflectarrays.

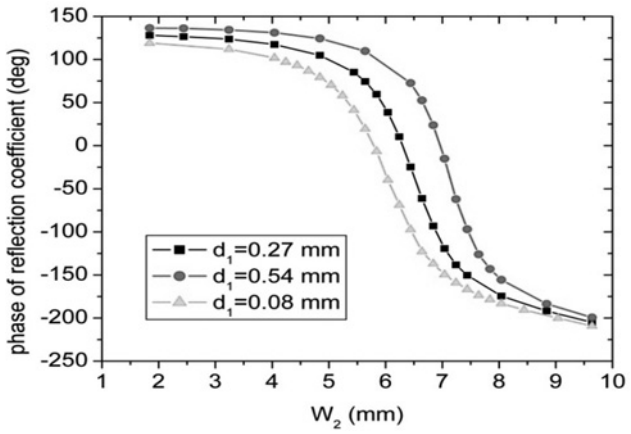

Fig. 7 *Phase of the reflected wave against length of the loop for different wire widths ($d_2 = 0.9$ mm) at 10.7 GHz*

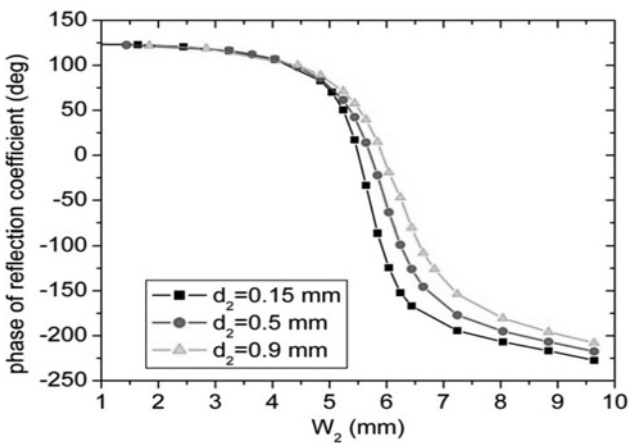

Fig. 8 *Phase of the reflected wave against loop length for different loop widths ($d_1 = 0.08$ mm) at 10.7 GHz*

Following the aforementioned design procedure, a prototype reflectarray antenna was designed and fabricated.

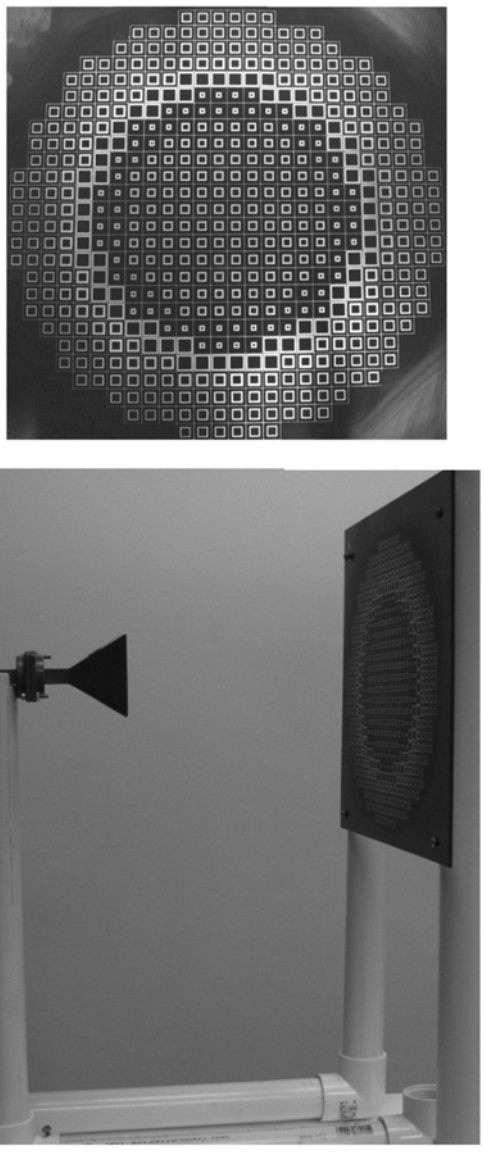

Fig. 9 *Photograph of the fabricated reflectarray antenna*

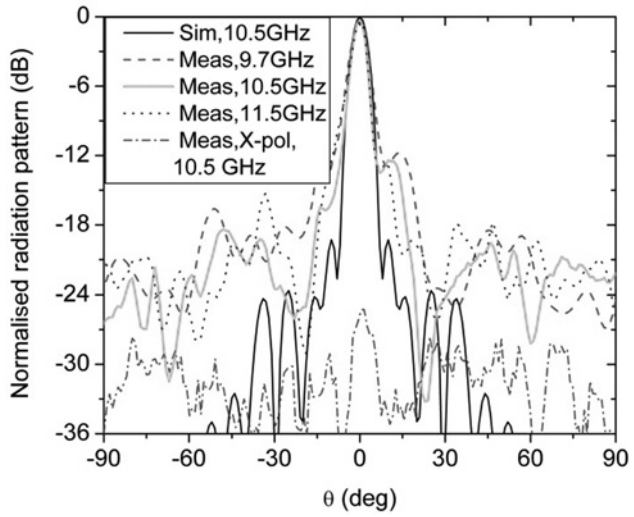

Fig. 10 *Measured radiation pattern of the reflectarray antenna*

In this design, the reflectarray antenna is centre fed with $F/D = 1.02$, with a broadside radiation. The photograph of the reflectarray is presented in Fig. 9. The substrate is Rogers RT/duroid 5880 with $\varepsilon_r = 2.2$ and $h = 3.175$ mm. An X-band horn antenna with dimensions of 88 mm × 65 mm was used as the feed and placed at a distance of about 26.5 cm from the reflector surface. The radiation patterns of the antenna at different frequencies are measured and compared with the full-wave simulation (using CST MWS) at the centre frequency and presented in Fig. 10. The 3 dB beamwidth of the antenna is 6° over the entire band and agrees well with the simulation. The discrepancy between the simulation and measured sidelobe levels is mainly because of the scattering from the coaxial cable and the supporting structure. Also the misalignment of the horn and the reflectarray surface in the fabricated prototype is another reason for the difference between the simulation and the measurement results. A typical plot of the measured cross-polarisation pattern of the antenna is also presented in Fig. 10. As it can be seen that the cross-polarisation level is about −25 dB below the co-polarisation level.

The gain of the antenna is measured and compared with the full-wave simulation and illustrated in Fig. 11. The maximum measured gain of 26.3 dBi at 10.5 GHz with a wide 1 dB gain–bandwidth of 17% is achieved which agrees well with the simulation result. The wide gain–bandwidth is attributed to the sub-wavelength dimension of the unit cell with high-order frequency response, large reflected phase span with a smooth phase against structural dimension variations and small variation of phase response to the various incident wave angles.

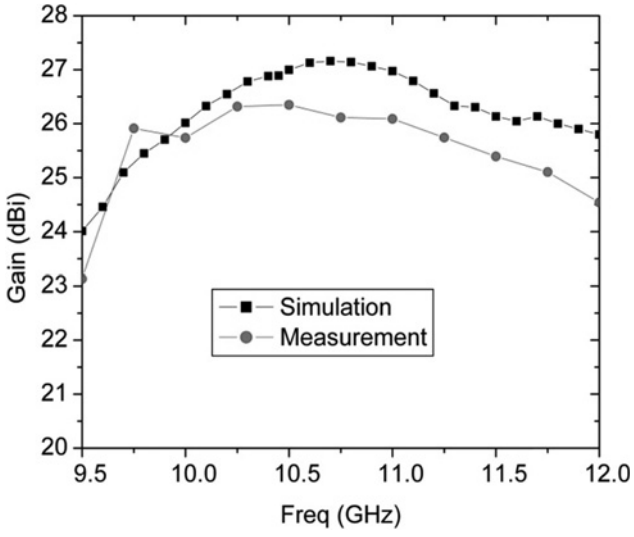

Fig. 11 *Measured and simulated gain of the reflectarray antenna*

4 Conclusion

A novel design of the reflectarray antenna based on the metal-backed loop-wire miniaturised-element FSS is proposed. It is shown that the proposed unit cell provides a larger phase range compared to the loop alone and a smooth phase variation against variation in the loop dimension. The latter relaxes stringent conditions on fabrication tolerance. In addition, the proposed unit cell shows low sensitivity to the wave angle of incidence and polarisation. An equivalent circuit model has been proposed for loop-wire element and experimental results based on waveguide measurements are used to validate the circuit model and the design procedure. It is shown because of the small size of the unit cells compared to the wavelength, the unit cells can be designed individually for the required phase shift, and placed in the appropriate location on the reflectarray. Full-wave simulations and experimental observations all indicate that no optimisation is required to achieve the desired radiation pattern. The aforementioned characteristics are the keys to achieve a wideband gain–bandwidth response. To validate the overall design procedure, a prototype reflectarray antenna was fabricated and measured. The antenna operates at the X-band and shows a gain of 26.3 dBi with 1 dB gain–bandwidth of 17% and 3 dB beamwidth of 6° across the band.

5 References

1 Rahmat-Samii, Y.: 'Reflector antennas', in Lo, Y.T., Lee, S.W. (Eds.): 'Antenna handbook' (Van Nostrand Reinhold, 1988), Ch. 15, pp. 15–1 and 15–124
2 Mailloux, R.J.: 'Phased array antenna handbook' (Artech house, 2005)
3 Berry, D.G., Malech, R.G., Kennedy, W.A.: 'The reflectarray antenna', *IEEE Trans. Antennas Propag.*, 1963, **11**, (6), pp. 643–651
4 Pozar, D.M., Metzler, T.A.: 'Analysis of reflectarray antenna using microstrip patches of variable size', *Electron. Lett.*, 1993, **29**, (8), pp. 657–658
5 Huang, J.: 'Reflectarray antennas' (Encyclopedia of Microwave Engineering, Wiley Online Library, 2005)
6 Huang, J.: 'Microstrip reflectarray'. IEEE Antennas and Propagation Symp., 1991, vol. 2, pp. 612–615
7 Huang, J., Encinar, J.A.: 'Reflectarray antennas' (Institute of Electrical and Electronics Engineers, John Wiley & Sons, 2008)
8 Encinar, J.A.: 'Design of two-layer printed reflectarrays using patches of variable size', *IEEE Trans. Antennas Propag.*, 2001, **49**, (10), pp. 1403–1410
9 Encinar, J.A., Zornoza, J.A.: 'Broadband design of three-layer printed reflectarrays', *IEEE Trans. Antennas Propag.*, 2003, **51**, (7), pp. 1662–1664
10 Bialkowski, M.E., Sayidmarie, K.H.: 'Investigations into phase characteristics of a single-layer reflectarray employing patch or ring elements of variable size', *IEEE Trans. Antennas Propag.*, 2008, **56**, pp. 3366–3372
11 Sayidmarie, K.H., Bialkowski, M.E.: 'Broadband microstrip reflectarray formed by double circular ring elements'. Int. Conf. Microwaves, Radar and Wireless Communications (MIKON), Wroclaw, May 2008, pp. 1–4
12 Mohammadirad, M., Komjani, N., Chaharmir, M.R., Shaker, J., Sebak, A.R.: 'The effect of feed position on the bandwidth performance of a broadband reflectarray'. IEEE AP-S Int. Symp., Spokane, July 2011, pp. 101–104

doi: 10.1049/iet-map.2013.0432

13 Chaharmir, M.R., Shaker, J., Cuhachi, M., Ittipiboon, A.: 'A broadband reflectarray antenna with double square rings', *Microw. Opt. Technol. Lett.*, 2006, **48**, (7), pp. 1317–1319
14 Moustafa, L., Gillard, R., Peris, F., Legay, H., Girard, E.: 'The phoenix cell: a new reflectarray cell with large bandwidth and rebirth capabilities', *IEEE Antennas Wirel. Propag. Lett.*, 2011, **10**, pp. 71–71
15 Pozar, D.M.: 'Wideband reflectarrays using artificial impedance surfaces', *Electron. Lett.*, 2007, **43**, (3), pp. 148–149
16 Nayeri, P., Yang, F., Elsherbeni, A.Z.: 'A broadband microstrip reflectarray using sub-wavelength patch elements'. Proc. IEEE Antennas Propagation Soc. Int. Symp., June 2009, pp. 1–4
17 Zhao, G., Jiao, Y.C., Zhang, F., Zhang, F.S.: 'A subwavelength element for broadband circularly polarized reflectarrays', *IEEE Antennas Propag. Lett.*, 2010, **9**, pp. 330–333
18 Misran, N., Cahil, R., Vusko, V.F.: 'Design optimization of ring elements for broadband reflectarray antenna', *IEE Proc.-Microw. Antennas Propag.*, 2003, **150**, (6), pp. 440–444
19 Ethier, J., Chaharmir, M.r., Shaker, J.: 'Reflectarray design comprised of sub-wavelength coupled-resonant square loop elements', *Electron. Lett.*, 2011, **47**, (22), pp. 1215–1217
20 Nayeri, P., Yang, F., Elsherbeni, A.Z.: 'Broadband reflectarray antennas using double layers sub-wavelength patch elements', *IEEE Antennas Wirel. Propag. Lett.*, 2010, **9**, pp. 1139–1142
21 Sarabandi, K., Behdad, N.: 'Frequency selective surface with minituarized elements', *IEEE Trans. Antennas Propag.*, 2007, **55**, (5), pp. 1239–1245
22 Bayatour, F., Sarabandi, K.: 'Multipole spatial filters using metamaterial-based miniaturized element frequency-selective surfaces', *IEEE Trans. Antennas Propag.*, 2008, **56**, (12), pp. 2742–2747
23 Marcuvitz, N.: 'Waveguide handbook' (Boston Technical Publishers, Lexington MA, 1964)
24 Sarabandi, K., Ulaby, F.T.: 'Technique for measuring the dielectric constant of thin materials', *IEEE Trans. Instrum. Meas.*, 1988, **37**, (4), pp. 631–636